SALL4, a novel oncogene, is constitutively expressed in human acute myeloid leukemia (AML) and induces AML in transgenic mice

Yupo Ma, Wei Cui, Jianchang Yang, Jun Qu, Chunhui Di, Hesham M. Amin, Raymond Lai, Jerome Ritz, Diane S. Krause, and Li Chai

***SALL4*, a human homolog to *Drosophila spalt*, is a novel zinc finger transcriptional factor essential for development. We cloned *SALL4* and its isoforms *(SALL4A* and *SALL4B).* Through immunohistochemistry and real-time reverse-transcription–polymerase chain reaction (RT-PCR), we demonstrated that *SALL4* was constitutively expressed in human primary acute myeloid leukemia (AML, n = 81), and directly tested the leukemogenic potential of constitutive expression of *SALL4* in a murine model. *SALL4B* transgenic mice developed myelodysplastic syndrome (MDS)–like features and subsequently AML that was transplantable. Increased apoptosis associated with dysmyelopoiesis was evident in transgenic mouse marrow and colony-formation (CFU) assays. Both isoforms could bind to β-catenin and synergistically enhanced the Wnt/β-catenin signaling pathway. Our data suggest that the constitutive expression of *SALL4* causes MDS/AML, most likely through the Wnt/β-catenin pathway. Our murine model provides a useful platform to study human MDS/AML transformation, as well as the Wnt/β-catenin pathway's role in the pathogenesis of leukemia stem cells. (Blood. 2006;108:2726-2735)**

Introduction

Myelodysplastic syndrome (MDS) is a hematologic disease marked by the accumulation of genomic abnormalities at the hematopoietic stem cell (HSC) level leading to pancytopenia, multilineage differentiation impairment, and bone marrow apoptosis.[1] Mortality in this disease results from pancytopenia or transformation to acute myeloid leukemia (AML). AML is a hematologic cancer characterized by the accumulation of immature myeloid precursors in the bone marrow and peripheral blood. From the analysis of chromosomal translocation in bone marrow samples from AML patients, it is clear that transcription factors critical for hematopoiesis play an important role in leukemogenesis.[2-5]

The pathogenesis of AML is considered to involve multistep genetic alternations.[6] Because only HSCs are considered to have the ability to self-renew, they are the best candidates for the accumulation of multistep, preleukemic genetic changes and transforming them into so-called leukemia stem cells (LSCs).[7-9] Alternatively, downstream progenitors can acquire self-renewal capacity and give rise to leukemia. A good example is the Wnt/β-catenin signaling pathway, which has been associated with the self-renewal of normal HSCs and the granulocyte-macrophage progenitors (GMPs) of chronic myeloid leukemia (CML).[10-15] LSCs are not targeted under current chemotherapy regimens and have been found to account for drug resistance and leukemia relapse.[8,9] Hunting for genes or signaling pathways involved in leukemia self-renewal will promote the development of more effective leukemia treatments.

The *SALL* gene family, *SALL1, SALL2, SALL3,* and *SALL4,* was originally cloned on the basis of its DNA sequence homology to *Drosophila spalt (sal).*[16-19] In *Drosophila*, *spalt* is a homeotic gene essential for development of posterior head and anterior tail segments. It plays an important role in tracheal development,[20] terminal differentiation of photoreceptors, and wing vein placement.[21] In humans, the *SALL* gene family is involved in normal development, as well as tumorigenesis.[19,22-27] *SALL* proteins belong to a group of C_2H_2 zinc finger transcription factors characterized by multiple finger domains distributed over the entire protein.[28] During the tracheal development of *Drosophila*, *spalt* is an activated downstream target of Wingless, a Wnt ortholog.[29] Of interest, Sato et al[30] demonstrated that *SALL1* interacted with β-catenin by functioning as a coactivator, suggesting that the interaction between *SALL* and the Wnt/β-catenin pathway was bidirectional.

We report here on the identification of *SALL4* isoforms and their constitutive expression in all human AML we examined. The direct impact of *SALL4* expression in AML was tested in vivo. We show that constitutive expression of *SALL4* in mice is sufficient to induce MDS-like symptoms and transformation to AML that is transplantable. We also demonstrate that *SALL4* is able to bind β-catenin and activate the Wnt/β-catenin signaling pathway. *SALL4* and β-catenin share similar expression patterns at different phases of CML. A potential mechanism accounting for the oncogenic role of *SALL4* in LSCs is proposed.

From the Division of Laboratory Medicine, Nevada Cancer Institute, Las Vegas; the Department of Pathology, Joint Program in Transfusion Medicine, Brigham and Women's Hospital/Children's Hospital Boston, Harvard Medical School, Boston, MA; the Department of Hematopathology, University of Texas M. D. Anderson Cancer Center, Houston; the Department of Laboratory Medicine and Pathology, University of Alberta, Edmonton, Canada; the Division of Hematologic Malignancies, Dana-Farber Cancer Institute, Harvard Medical School, Boston, MA; and the Department of Laboratory Medicine, Yale University School of Medicine, New Haven, CT.

Submitted February 3, 2006; accepted May 24, 2006. Prepublished online as *Blood* First Edition Paper, June 8, 2006; DOI 10.1182/blood-2006-02-001594.

Supported in part by the National Institutes of Health under grants K08 CA097185 and P20 RR016464 (Y.M.) and K08 DK063220, and by the National Blood Foundation (L.C.).

Reprints: L. Chai, Department of Pathology, Brigham and Women's Hospital, Harvard Medical School, 75 Francis St, Boston, MA 02115; e-mail: lchai@partners.org; Y. Ma, Division of Laboratory Medicine, Nevada Cancer Institute, 10441 W Twain Avenue, Las Vegas, NV 89135; e-mail: yma@nvcancer.org.

The publication costs of this article were defrayed in part by page charge payment. Therefore, and solely to indicate this fact, this article is hereby marked "advertisement" in accordance with 18 U.S.C. section 1734.

Materials and methods

Molecular cloning

Plasmid construction and DNA sequencing were performed in accordance with standard procedures. For cloning of *SALL4* isoforms, polymerase chain reaction (PCR) primers were designed, based on the genomic clone RP5-1112F19 (GenBank accession no. AL034420). *SALL4* isoforms were cloned with the use of the Marathon-Ready cDNA library derived from human fetal kidney (BD Biosciences Clontech, Palo Alto, CA), according to the supplier's protocol. The amplified PCR products were cloned into a TA Cloning vector (Invitrogen, Carlsbad, CA), and the nucleotide sequences were determined by DNA sequencing.

Determination of *SALL4* alternative splicing patterns in different tissues and Wnt/β-catenin downstream target gene expression (c-Myc and Cyclin D1)

Reverse transcription (RT)–PCR was used to evaluate mRNA expression patterns of *SALL4* in adult tissues. A panel of 8 normalized first-strand cDNA preparations, derived from different adult tissues, was purchased from BD Biosciences Clontech. PCR amplification was performed in a 50-μL reaction volume containing 5 μL cDNA, 10 mM Tris HCl (pH 8.3), 50 mM KCl, 2 mM $MgCl_2$, 0.2 mM dNTPs, and 1.25 U Taq DNA polymerase (PerkinElmer Life Sciences, Boston, MA). After an initial denaturation at 94°C for 10 minutes, amplification was performed for 30 cycles under the following conditions: 30-second denaturation at 94°C, 30-second annealing at 55°C, and 30-second extension at 72°C. The last cycle was followed by a final 7-minute extension at 72°C. Amplification of glyceraldehyde phosphate dehydrogenase (GAPDH) mRNA was used to control for template concentration loading. The primer pairs for *SALL4* isoforms were the following: primer A1, 5′-TCCGAGAACAGCCGCACTGAGATGGAAG-3′; primer B1, 5′-GTTCACTACATGACACACGGGGCG-3′; primer C1, 5′-ATGTCGAGGCGCAAGCAGGCGAAAC-3′; and primer D1, 5′-TTAGCTGACCGCAATCTTGTTTTCTTCC-3′. PCR products were electrophoretically separated on 1% agarose gel. DNA sequencing was also used to confirm amplification products. To determine the expressions of Wnt/β-catenin downstream target genes, RT-PCR was also used on bone marrow samples from wild-type control, and preleukemic and leukemic *SALL4B* transgenic mice. The primers for c-Myc were as follows: forward, 5′-TTT GTC TAT TTG GGG ACA GTG TT-3′; reverse, 5′-CAG CTT CTC CGA GAC CAG CTT GGC AGC-3′. The primers for Cyclin D1 were as follows: forward, 5′-CCT CTC CTG CTA CCG CAC AAC GCA C-3′; reverse, 5′-CTC TCA GGG TGA TGC AGA TTC TAT CTC-3′. Beta actin was used as a control; its primers were as follows: forward, 5′-GAC GAG GCC CAG AGC AAG AGA GG-3′; reverse, 5′-GTG ATG ACC TGG CCG TCA GGC AG-3′.

Antibody generation

The peptide MSRRKQAKPQHIN of human *SALL4* was chosen for its potential antigenicity (amino acids 1-13) and used to prepare an antipeptide antibody. This region is also identical to that of mouse *SALL4* so that the generated antibody could be expected to cross-react with mouse *SALL4*. *SALL4* antipeptide antibody was produced in rabbits in collaboration with Lampire Biological Laboratories (Pipersville, PA).

Gel electrophoresis and Western blot analysis

Sodium dodecyl sulfate–polyacrylamide gel electrophoresis (SDS-PAGE) was carried out in SDS 10% wt/vol polyacrylamide slab gels according to Laemmli, and the proteins were then transferred to nitrocellulose membranes. Immunoblotting of rabbit immune serum with the *SALL4* antipeptide antibody (1:100) was performed with an electrochemiluminescence detection system as described by the manufacturer (Amersham Biosciences, Piscataway, NJ).

Leukemia and normal tissues

Leukemia and normal samples, either in paraffins or frozen in dimethylsulfoxide (DMSO), were collected from the files of the University of Texas M. D. Anderson Cancer Center (Houston) and the Dana-Farber Cancer Institute (Boston, MA), between 1998 and 2004 under approved institutional review board protocols. The diagnosis of all tumors was based on morphologic and immunophenotypic criteria according to the French-American-British (FAB) Classification for Hematopoietic Neoplasms. $CD34^+$ fresh cells were purchased from Cambrex (Walkersville, MD).

Real-time quantitative RT-PCR

We used the TaqMan 5′ nuclease assay (Applied Biosystems, Foster City, CA) in these studies. Total RNA from purified $CD34^+$ HSCs/hematopoietic progenitor cells (HPCs) from normal bone marrow and peripheral blood, 15 AML samples, and 3 leukemia cell lines were isolated with the RNeasy Mini Kit and digested with DNase I (Qiagen, Valencia, CA). RNA (1 μg) was reverse-transcribed in 20 μL with the use of Superscript II reverse transcriptase and a poly(dT)12-18 primer (Invitrogen). After the addition of 80 μL water and mixing, 5-μL aliquots were used for each TaqMan reaction. TaqMan primers and probes were designed with the use of Primer Express software version 1.5 (Applied Biosystems). Real-time PCR for *SALL4* and GAPDH was performed with the TaqMan PCR core reagent kit (Applied Biosystems) and an ABI Prism 7700 Sequence Detection System (Applied Biosystems). The PCR reaction mixture contained 3.5 mM $MgCl_2$; 0.2 mM each of deoxyadenosine triphosphate (dATP), deoxycytidine triphosphate (dCTP), and deoxyguanosine triphosphate (dGTP); 0.4 mM deoxyuridine triphosphate (dUTP); 0.5 μM forward primer; 0.5 μM reverse primer; 0.1 μM TaqMan probe; 0.25 U uracil DNA glycosylase; and 0.625 U AmpliTaq Gold polymerase in 1 × TaqMan PCR buffer. cDNA (5 μL) was added to the PCR mix, and the final volume of the PCR reaction was 25 μL. All samples were run in duplicate. GAPDH was used as an endogenous control. Thermal cycler conditions were 50°C for 2 minutes, 95°C for 10 minutes, and 45 cycles of 95°C for 0.30 minutes and 60°C for 1 minute. Data were analyzed with the use of Sequence Detection System software version 1.6.3 (Applied Biosystems). Results were obtained as threshold cycle (Ct) values. The software determines a threshold line on the basis of the baseline fluorescent signal, and the data point that meets the threshold is given as the Ct value. The Ct value is inversely proportional to the starting number of template copies. All measurements were performed in duplicate. TaqMan sequences include the following: GAPDH forward primer (5′-GAAGGTGAAGGTCGGAGTC-3′) and reverse primer (5′-GAAGATGGTGATGGGATTTC-3′); TaqMan probe (5′-CAAGCTTCCCGTTCTCAGCC-3′); *SALL4A* forward primer (5′-TGCAGCAGTTGGTGGAGAAC-3′) and reverse primer (5′-TCGGTGGCAAATGAGACATTC-3′); and *SALL4B* forward primer (5′-ACATCTCCGCGGTGGATGT-3′) and reverse primer (5′-TGCTCCGACACTTGTGCTTG-3′).

Design and construction of tissue arrays

Tissue arrays that included triplicate tumor cores from leukemia specimens were sectioned (5-μm thick). A manual tissue arrayer (Beecher Instruments, Silver Spring, MD) was used to construct the tissue arrays.

Immunohistochemistry

Immunohistochemical staining was performed according to standard techniques. Briefly, formalin-fixed, paraffin-embedded, 4-μm–thick tissue sections were deparafinized and hydrated. Heat-induced epitopes were retrieved with a Tris buffer (pH 9.9; Dako, Carpinteria, CA) and a rapid microwave histoprocessor. After incubation at 100°C for 10 minutes, slides were washed in running tap water for 5 minutes and then with phosphate-buffered saline (PBS; pH 7.2) for 5 minutes. Tissue sections were then incubated with anit-*SALL4* antibody (1:200) for 5 hours in a humidified chamber at room temperature. After 3 washes with PBS, tissue sections were incubated with anti–mouse immunoglobulin G and peroxidase for 30 minutes at room temperature. After 3 washes with PBS, tissue sections were incubated with 3,3′-diaminobenzidine/H_2O_2 (Dako) for color development; hematoxylin was used to counterstain the sections. Cells were considered to be positive for *SALL4* when they showed definitive nuclear staining.

Image acquisition

Images were visualized using an Olympus BH-2 microscope (Olympus, Tokyo, Japan), equipped with one of the following: a Dplan4 4×/0.10 numeric aperture (NA) air objective (Figures 2Bv, 4Bviii); an Splan10 10×/0.3 NA air objective (Figures 4Bii,v); an Splan 20 20×/0.46 NA air objective (Figure 4Diii-vi and 5Ai,ii); an Splan40 40×/0.70 NA air objective (Figures 2Bi-iv,vi, 4Biii,vi, and 4Bviii inset); or an Splan Apo60 60×/1.4 NA oil objective (Figures 4Ai-xvi, 4Bi,iv, 5Bi-iv; microscope immersion oil from Richard-Allan Scientific, Kalamazoo, MI). All micrographs were visualized using hematoxylin and eosin stain. All images including the gross-view pictures (Figures 4Bvii, 4Di-ii) were taken at room temperature using an Olympus Q-color 5 camera (model 32-0055B-128) and were processed using Adobe Photoshop (Adobe Systems, San Jose, CA).

Generation of transgenic mice

SALL4B cDNA, corresponding to the entire coding region, was subcloned into a pCEP4 vector (IntroGene; now Crucell, Leiden, The Netherlands) to create the cytomegalovirus (CMV)/*SALL4B* construct for the transgenic experiments. Subsequent digestion with *Sal*I, which does not cut within the *SALL4B* cDNA, released a linear fragment containing only the CMV promoter, the *SALL4* cDNA coding region, the simian virus 40 (SV40) intron, and polyadenylation signal without additional vector sequences.

Transgenic mice were generated via pronuclear injection performed in the transgenic mouse facility at Yale University. Identification of *SALL4B* founder mice and transmission of the transgene was determined by PCR analyses. Tissue expressions of transgene were confirmed by RT-PCR. The PCR primers used for the RT-PCR span the junction of the 5′ *SALL4B* cDNA to the CMV promoter (sense primer, 5′-CAG AGA TGC TGA AGA ACT CCG CAC-3′; antisense primer, 5′-AGC AGA GCT CGT TTA GTG AAC CG-3′).

Hematologic analysis

Complete blood cell counts with automated differentials were determined with a Mascot Hemavet cell counter (CDC Technologies, Oxford, CT). For progenitor assays, 1.5×10^4 bone marrow cells were plated in duplicate 1.25-mL methylcellulose cultures supplemented with recombinant mouse interleukin-3 (IL-3, 10 ng/mL), IL-6 (10 ng/mL), stem cell factor (SCF; 50 ng/mL), and erythropoietin (3 U/mL) (M3434; StemCell Technologies, Vancouver, BC). Colonies were recorded between days 7 and 14 (colony-forming unit–granulocyte [CFU-G], CFU–granulocyte-macrophage [CFU-GM], CFU-macrophage [CFU-M], CFU–granulocyte-erythrocyte-megakaryocyte-macrophage [CFU-GEMM], and burst-forming unit–erythroid [BFU-E]). Peripheral blood, bone marrow smears, and cytospin from pooled CFU cells were stained with Wright-Giemsa stain.

Flow cytometric analysis

Cells were stained with directly conjugated antibodies to Gr-1, Mac-1, B220, Ter119, c-kit, CD34, CD45, CD41, CD19, CD5, CD3, CD4, CD8, propidium iodide (PI), or annexin V (BD Biosciences Pharmingen, San Diego, CA). Ten thousand scatter-gated live cells were acquired on a FACScan and analyzed with CellQuest software (BD Biosciences Clontech).

Statistical analysis

Student *t* test was used for all the statistical analyses, assuming normal 2-tailed distribution and unequal variance.

Cell culture

HEK-293 cells (derived from human embryonic kidney) and cell lines KG.1 (derived from human acute myeloid leukemia), Kasumi-1 (derived from human myeloid leukemia AML-M2), and THP-1 (derived from human promonocytic leukemia AML-M4/M5) were purchased from the American Type Culture Collection (Manassas, VA). Cells were maintained at 37°C in a humidified environment with 5% carbon dioxide and 10% fetal serum.

Transfection

Transfection was performed with Lipofectamine 2000 reagent (Invitrogen) according to the manufacturer's instructions. Cells were plated in 24-well plates at a density of approximately 1×10^5 cells/well. Cells were harvested 24 hours after transfection. Plasmid DNA for transient transfection was prepared with the Qiagen Plasmid Midi Kit.

β-Galactosidase and luciferase assays

The cells were extracted with 100 μL luciferase cell culture lysis reagent (Promega, Madison, WI) 24 hours after transfection. The β-galactosidase assay, performed with 15 μL cell extract, used the β-Galactosidase Enzyme Assay System (Promega) and the standard assay protocol provided by the manufacturer (except that 1 M Tris base was used as stopping buffer, instead of sodium carbonate). For the luciferase assay (Promega), 20 μL extract were used in accordance with the manufacturer's instructions. After subtraction of the background, luciferase activity (arbitrary units) was normalized to β-galactosidase activity (arbitrary units) for each sample.

Results

Molecular cloning of 2 alternatively splicing isoforms of human *SALL4*

Two full-length transcripts of *SALL4* were isolated by 5′ and 3′ RACE-PCR (rapid amplification of the 5′ and 3′ cDNA ends–polymerase chain reaction) with the use of fetal human kidney Marathon-Ready cDNAs (BD Biosciences Clontech) as templates. Sequence analysis of the larger cDNA fragment isolated revealed a single, large open-reading frame, designated as *SALL4A,* that started from a strong consensus initiation sequence and was expected to encode 1053 amino acids. The other splicing variant of *SALL4,* designated *SALL4B,* lacked the region corresponding to amino acids 385 to 820 of the full-length *SALL4A* (Figure 1A). The putative protein encoded by *SALL4B* cDNA was expected to consist of 617 amino acids.

To rule out the possibility that these 2 apparent splicing variants might result from artifacts, we compared both variant mRNA sequences with corresponding sequences of the human genome. *SALL4A* contained all exons (1-4) (Figure 1A), whereas *SALL4B* lacked a large portion of the 3′ end of exon 2. Both exon-intron splice sites satisfied the G-T-A-G rule. Both splicing variants had the same translational reading frame, but *SALL4B* mRNA encoded a protein with internal deletion. *SALL4A* contained 8 zinc finger domains, while *SALL4B* had 3 zinc finger domains.

Expression pattern of the *SALL4* isoforms in human tissues

The alternative splicing patterns of *SALL4* were delineated by RT-PCR in a variety of human tissues. A fragment of the ubiquitous GAPDH gene cDNA was amplified as a control (Figure 1B). A 315-bp fragment representing the longer splice variant, *SALL4A,* was amplified in some tissues, achieving various expression levels. The *SALL4B* variant was present in every tissue at varying levels of expression.

Generation of *SALL4* antibody and identification of *SALL4* protein products

To identify *SALL4* gene products and confirm the presence of *SALL4* variants, we developed a polyclonal antibody against a synthetic peptide (amino acids 1-13) of *SALL4.* This region was chosen because it is common to both *SALL4* variants. The

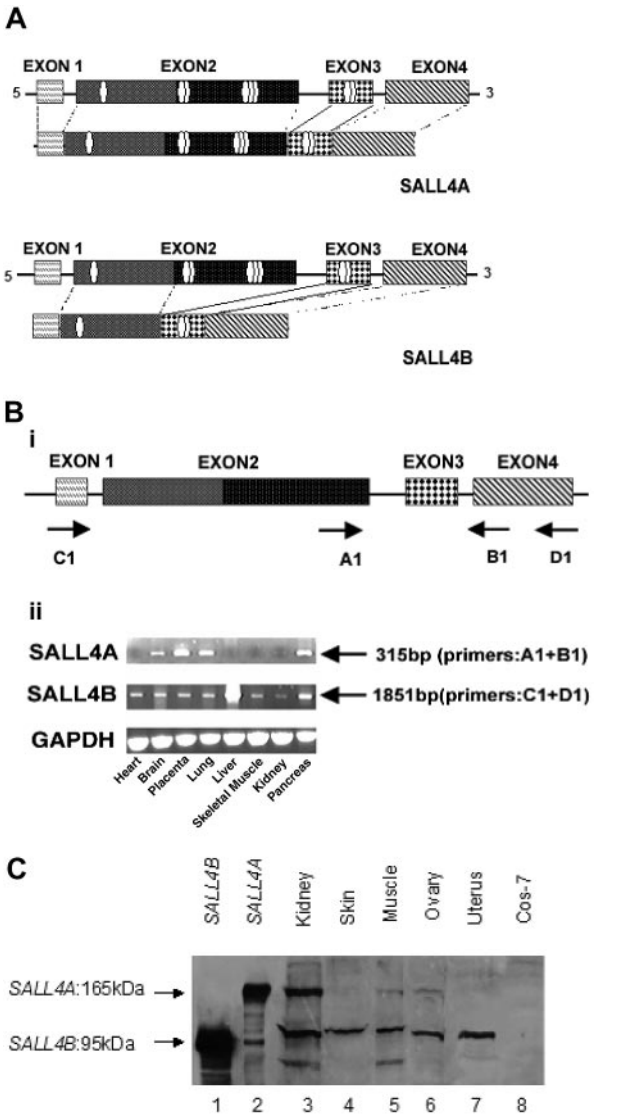

Figure 1. *SALL4* has 2 isoforms. Alternative splicing generates 2 variant forms of *SALL4* mRNA. (A) *SALL4A* and *SALL4B* vary in protein length and in the presence of different numbers of characteristic *sal*-like zinc finger domains. *SALL4A* (encoding 1067 amino acids) contains 8 zinc finger domains, while *SALL4B* (encoding 623 amino acids) has 3 zinc finger domains. Both variants have exons 1, 3, and 4, and *SALL4A* contains all exons from 1 to 4. However, *SALL4B* uses an alternative splice donor that results in deletion of the large 3′ portion of exon 2. (B) RT-PCR analysis of *SALL4* variants in different human tissues. Four exons of *SALL4* and their potential coding structures are illustrated, with arrows indicating the primers used for PCR amplification of the *SALL4* transcripts (i). Tissue-dependent expression of *SALL4* transcripts by RT-PCR (ii). A 315-bp expected product that was specific for *SALL4A* with primers A1 (exon 2) and B1 (exon 4) was amplified with cDNAs of various tissues. Primers D1 (exon 4) and C1 (exon 1) were used to amplify the 1851-bp expected product of *SALL4B*. Comparable amounts of cDNA were determined by GAPDH. (C) *SALL4* protein products, *SALL4A*, and *SALL4B* identified by a *SALL4* peptide antibody. Lysates from Cos-7 cells transiently expressing His-*SALL4B* (lane 1), His-*SALL4A* (lane 2), or control vector (lane 8), or lysates from different human tissues were resolved by 10% SDS-PAGE gel, transferred onto a nitrocellulose membrane, and probed with the N-terminal *SALL4* peptide antibody.

affinity-purified *SALL4* peptide antibody recognized specifically 2 endogenous proteins in a human kidney total lysate. The 2 proteins were approximately 165 kDa and 95 kDa, which were identical to the apparent molecular weights of overexpressed *SALL4A* and *SALL4B* in Cos-7 cells, respectively (Figure 1C). Western blotting with this antibody confirmed that the *SALL4* isoforms had different tissue distributions (Figure 1Dii).

Constitutive expression of *SALL4* mRNA in human primary AML and myeloid leukemia cell lines

Because another *SALL* gene family member *SALL2* is involved in tumorigenesis, we examined *SALL4* mRNA expression in AML. Expression of *SALL4* was quantitatively investigated by real-time RT-PCR in bone marrow cells derived from AML samples (n = 15) and myeloid leukemia cell lines (n = 3) and compared with that of nonneoplastic hematopoietic cells from a purified $CD34^+$ stem/progenitor pool (HSCs/HPCs purchased from Cambrex), normal bone marrow (n = 3), and normal peripheral blood (n = 3). With the use of isoform-specific primers (Figure 2A), we observed that during normal hematopoiesis, both *SALL4* isoforms were down-regulated. In contrast, both *SALL4A* and *SALL4B* mRNA levels were constitutively expressed in 60% of AML samples and in all 3 cell lines. In the remaining 40% of AML samples, either *SALL4A* or *SALL4B* was constitutively expressed. Compared with normal hematopoiesis cells, leukemia samples had a wide range of *SALL4A* or *SALL4B* expression levels. This is probably due to the fact that the leukemia samples had a variable range of leukemic blasts population (40%-90%).

Constitutive expression of *SALL4* protein in human primary AML

To investigate whether the observed aberrant *SALL4* expression was also present at the protein level, we examined 81 AML samples, ranging from AML subtypes M1 to M5 (FAB classification): M1 (n = 20), M2 (n = 27), M3 (n = 8), M4 (n = 16), M5 (n = 3), and AML nonspecified (n = 7); and several samples of normal bone marrow, thymus, and spleen, as well as normal $CD34^+$ HSCs/HPCs.

Normal bone marrow, spleen, and thymus showed no detectable *SALL4* protein expression, and $CD34^+$ HSCs/HPCs exhibited positive but weaker *SALL4* protein staining; however, much stronger *SALL4* expression was detected in the nuclei of leukemic cells (Figure 2Bvi). All 81 AML samples showed aberrant *SALL4* expression, which was consistent with *SALL4* mRNA expression levels demonstrated by real-time RT-PCR (Figure 2A). The strongest staining was seen in AML-M1 and -M2. Our data suggested that *SALL4* was present in $CD34^+$ HSCs/HPCs and down-regulated in mature granulocytes and lymphocytes. As a result, the constitutive expression of *SALL4* in leukemia may have prevented the leukemic blasts from differentiating and/or gaining properties that were normally seen in HSCs, probably by interacting with additional mutations since leukemogenesis is a multistep pathologic process.

Generation of transgenic mice constitutively expressing full-length human *SALL4B*

To directly test whether constitutive expression of *SALL4* is sufficient to induce AML, we generated a *SALL4* transgenic mouse model. The CMV promoter was fused to cDNA that encoded the 617 amino acids of human *SALL4B* (Figure 3A), which was chosen because it was expressed in every tissue previously examined (Figure 1Dii). The CMV promoter was previously used to ectopically express human genes in most murine organs. RT-PCR amplification was performed to examine the expression of wild-type (WT), full-length *SALL4B* in the transgenic mice. A *SALL4B* transcript was detected in a variety of tissues from the transgenic mice, including brain, kidney, liver, spleen, lymph nodes, peripheral blood, and c-kit–positive population in the bone marrow (Figure 3B). Abnormal gaits and associated hydrocephalus 3 weeks after birth were observed in 20% of the transgenic mice from multiple lines; 60% had polycystic kidneys.

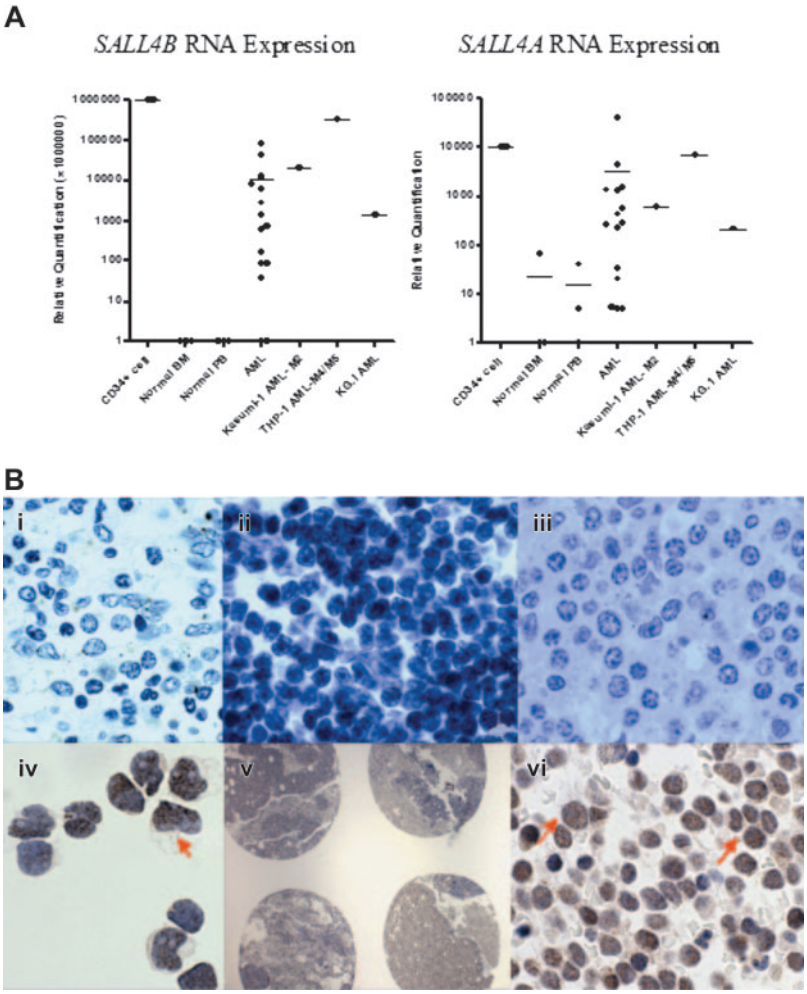

Figure 2. *SALL4* expression in human primary AML and myeloid leukemia cell lines. (A) *SALL4* mRNA expression in AML. Real-time PCR quantification of *SALL4A* and *SALL4B* normalized to GAPDH showed that both *SALL4A* and *SALL4B* were expressed in purified CD34$^+$ cells, but *SALL4A* was rapidly down-regulated and *SALL4B* turned off in normal bone marrow (n = 3) and normal peripheral blood (n = 3) cells. In contrast, in 15 primary AML samples and 3 myeloid leukemia cell lines (Kasumi-1, THP-1, and KG.1), the expression of *SALL4A* or *SALL4B*, or both, failed to be down-regulated. The results were calibrated against the expression of *SALL4A* or *SALL4B* in purified CD34$^+$ cells. Y-axis: Log scale on the relative quantification. (B) Constitutive expression of *SALL4* protein in human AML (FAB M1-M5, n = 81) is demonstrated by immunohistochemical staining. No *SALL4* expression was detected in normal bone marrow (i), normal thymus (ii), or normal spleen (iii). All cell nuclei remained blue. Nuclei of CD34$^+$ HSCs/HPCs showed brown staining indicating *SALL4* expression (iv); acute myeloid leukemia blasts showed similar staining (v, low power [× 4]) in microarray leukemia tissue samples. Each circle represents one leukemia sample. (vi) High-power (× 400) view of one leukemia sample shown in panel vii. The red arrows indicate positive nuclear staining.

MDS-like features and AML in *SALL4B* transgenic mice

Monitoring of hematologic abnormalities in a cohort of 16 transgenic mice from all 6 lines revealed that all mice had apparent MDS-like features at ages 6 to 8 months. Increased number of immature blasts and many atypical and dysplastic white cells, including hypersegmented neutrophils and pseudo-Pelger-Huet–like cells, were seen on peripheral blood smears (Figure 4A). Nucleated red blood cells and giant platelets were also present, as well as erythroid and megakaryocyte dysplastic features, such as binucleate erythroid precursors and hypolobulated megakaryocytes.

Eight (50%) of these 16 mice eventually progressed to acute leukemia (Table 1). Leukemic infiltration of many organs, including lungs, kidneys, liver, spleen, and lymph nodes, emphasized the aggressiveness of the disease (Figure 4B). Leukemia blast cells were CD34$^+$, and considered to be myeloid in origin because they were positive for c-kit, Gr-1, Mac-1, and myeloperoxidase; they were negative for B-cell (B220 and CD19), T-cell (CD4, CD8, CD3, and CD5), megakaryocytic (CD41), and erythroid (Ter119) markers (Figure 4C).

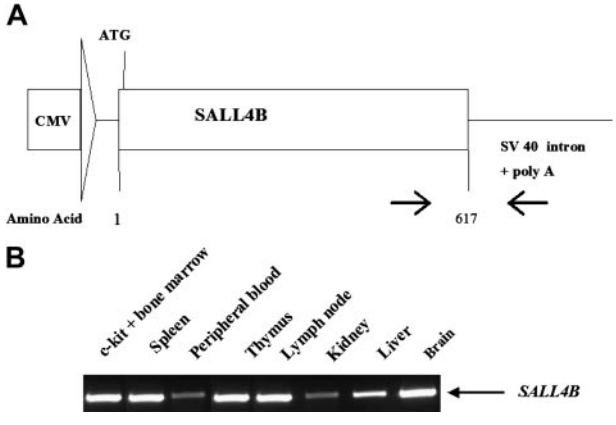

Figure 3. Generation of *SALL4B* transgenic mice. CMV/*SALL4B* transgenic construct and PCR analysis of transgenic line 507. (A) Schematic diagram of transgenic construct. The approximately 1.8-kb cDNA of *SALL4B* was subcloned into a pCEP4 vector, and the CMV/*SALL4* construct was excited by digestion with *Sal*I. (B) Tissue distribution of *SALL4B* in transgenic mice. The location of primers used for RT-PCR amplification is indicated by arrows in panel A. A primer specific for human *SALL4B* at the C-terminus was used as a 5′ primer, in combination with SV40-noncoding sequence-specific primers for RT-PCR of various tissues.

SALL4B-induced AML was transplantable

Aggressive fatal AML with onset at approximately 6 weeks developed in immunodeficient NOD/SCID mice after serial transplantation of *SALL4B*-induced AML cells by subcutaneous injection. The transplanted disease was positive for c-Kit and characterized by dissemination to multiple organs, with marked splenomegaly and hepatomegaly (Figure 4D). *SALL4B* expression was detectable in transplanted leukemic cells (data not shown).

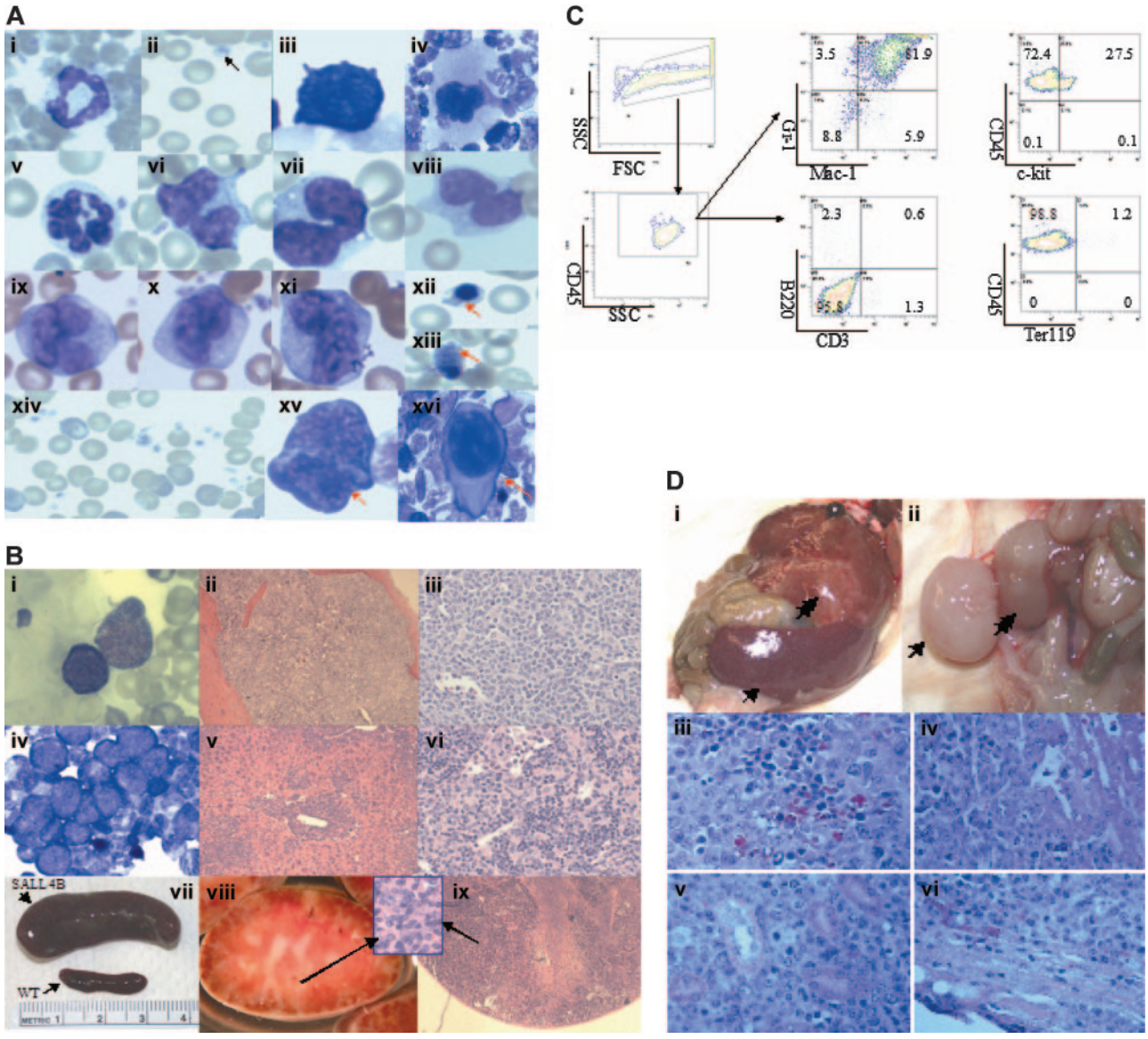

Figure 4. *SALL4B* transgenic mice have an MDS-like/AML phenotype. (A) MDS-like changes in *SALL4B* transgenic mice. Giemsa staining of peripheral blood from normal, age-matched WT littermates showed normal neutrophils (i), and normal red blood cells and platelets (ii, black arrow). In transgenic mice, neutrophils were hypersegmented (v), and pseudo-Pelger-Huet–like atypical white cells were present (vi-viii), together with increased numbers of immature cells (ix-xi). Nucleate red cells (xii, red arrow), giant platelets (xiii, red arrow), and polychromasia (xiv) were also observed in the transgenic mice. A binucleate dysplastic erythrocyte (xv, red arrow) and a dysplastic megakaryocyte with a hypolobulated nucleus (xvi, red arrow) were found in the cytospin from transgenic mouse bone marrow. An erythroid precursor (iii) and a megakaryocyte (iv) from WT control animals are shown for comparison. (B) AML (AML is defined as blast count more than 20% in peripheral blood and/or bone marrow with multiple organ involvements) observed in *SALL4B* transgenic mice (mouse 25). Blasts were present in the peripheral blood (i, × 600), bone marrow biopsy specimen (ii, × 100; iii, × 400), bone marrow smear (iv, × 600), liver (v, × 100), lymph node (vi, × 400), and spleen (vii-viii, gross view; ix, × 100; and the inset, × 400). (C) Flow cytometric analysis of leukemia in *SALL4B* transgenic mice. Leukemia cells from bone marrow, spleen, and lymph nodes were positive for CD45 and myeloid markers such as c-kit, Gr-1, and Mac-1, and negative for B cells (B220), T cells (CD3), and erythrocytes (Ter119). Numbers in quadrants indicate the percentage of total cells. (D) Serial transplantation of *SALL4B*-induced AML to NOD/SCID mice. Gross picture (i-ii) and histology (iii-vi, × 200) on splenomegaly (i [black arrow], iii), hepatomegaly (i [double black arrows], iv), lymph node enlargement (ii [black arrow], v), and pale kidney (ii [double black arrows], vi) caused by leukemia infiltration in a NOD/SCID mouse 6 weeks after leukemia transplantation.

Ineffective hematopoiesis and excessive apoptosis in *SALL4B* transgenic mice

Investigation of hematologic abnormalities in younger *SALL4B* transgenic mice (2-6 months old) revealed that their peripheral blood showed minimal myelodysplastic features but statistically significant leukopenia and neutropenia, as well as mild anemia (Table 2). To determine whether the cause of cytopenia in these transgenic mice was related to ineffective hematopoiesis, we studied their bone marrow. Bone marrow samples showed increased cellularity and an increased myeloid population (Figure 5A), compared with those of WT controls (Gr-1/Mac-1 double-positive population in *SALL4B* transgenic mice: 67% ± 16% [n = 10] vs WT: 55.3% ± 4% [n = 11]; $P = .048$).

As excessive apoptosis plays a central role in ineffective hematopoiesis in human MDS, we next examined apoptosis in *SALL4* transgenic mice in vivo and in vitro. Increased apoptosis was observed in *SALL4B* transgenic mice on both primary bone marrow (annexin V–positive, PI-negative population in transgenic mice: 11% ± 4.48% [n = 10] vs WT: 6.15% ± 4.98% [n = 7]; $P = .03$) and day-7 CFUs (annexin V–positive, PI-negative population in transgenic mice: 20.1% ± 6% [n = 10] vs WT: 10.9% ± 4% [n = 7]; $P = .002$) (Figure 5A-B). These findings

Table 1. Summary of MDS-like/AML in *SALL4B* transgenic mice

Mouse ID	Sex	Founder	Age, mo	Phenotype	Outcome and organs involved by AML*
464	M	464	19	MDS-like	Died of MDS
4	M	464	22	MDS-like	Alive
504	M	504	19	MDS-like	Killed due to MDS
86	F	504	18	AML	Killed; AML in BM, PB, liver, spleen, LNs
87	F	504	8	AML	Killed; AML in BM, PB, liver, spleen, LNs
506	M	506	19	MDS-like	Killed due to MDS
1336	F	506	14	AML	Killed; AML in BM, liver, spleen, LNs
2548	F	506	14	AML	Killed; AML in BM, liver, spleen
507	F	507	24	AML	Died; AML in BM, PB, liver, spleen, LNs
23	M	507	22	MDS-like	Killed due to MDS
25	M	507	8	AML	Killed; AML in BM, PB, liver, spleen, LNs
26	M	507	14	MDS	Killed due to MDS
27	M	507	22	MDS-like	Alive
3058	F	507	12	AML	Died; AML in BM, PB, liver, spleen and LNs
509	F	509	18	AML	Killed; AML in BM, PB, liver, spleen, LNs, lung
510	F	510	24	MDS-like	Killed due to MDS

*Mice were killed when noticed to be ill. AML is defined to have more than 20% c-kit-positive immature cells in the bone marrow or peripheral blood, with leukemia cells involving multiple organs.

may account for the fact that despite an increased myeloid population in bone marrow, these transgenic mice had statistically significant low neutrophil counts in the peripheral blood, secondary to an ongoing ineffective myelopoiesis in their bone marrow. An increased population of immature cells was also noted in *SALL4B* transgenic mice on both primary bone marrow (c-kit–positive population in *SALL4B* transgenic mice: 10.2% ± 1.3%, [n = 14] vs WT: 6.5% ± 2.5% [n = 10]; $P = .008$) (Figure 5A) and day-7 CFUs ($CD34^+$ population in *SALL4B* transgenic mice: 11% ± 2.2% [n = 8] vs WT: 6.3% ± 2.4% [n = 7]; $P = .002$) (Figure 5B). Similar numbers of total colonies were observed in *SALL4B* transgenic mice and WT controls (total colonies in *SALL4B* mice: 42 ± 29.5 [n = 10] vs WT: 39 ± 13.5 [n = 6]; $P = .23$). Statistically significant increased myeloid (CFU-GM in *SALL4B* transgenic mice: 53.6 ± 10.3 [n = 13] vs WT: 38.1 ± 3.1 [n = 8]; $P = .002$) and decreased erythroid (BFU-E in *SALL4B* transgenic mice: 7.8 ± 3.8 [n = 13] vs WT: 14.1 ± 2.7 [n = 8]; $P = .001$) colony populations (Figure 5Cii), however, were found in *SALL4B* transgenic mouse CFUs compared with those of WT controls, as has been reported in human MDS patients and other MDS mouse models.[31-35] These observations suggest that the defect in *SALL4B* transgenic mice lies at the stem cell/progenitor level affecting hematopoietic differentiation.

Binding of *SALL4A* and *SALL4B* to β-catenin in vitro

We next explored the potential signaling pathway that *SALL4* may affect in leukemogenesis. In *Drosophila*, Wnt signaling controls *spalt (sal)* expression during tracheal morphogenesis. *SALL1,* another member of the *SALL* gene family, can interact with β-catenin. The high-affinity site for this interaction is located at the C-terminal double zinc finger domain. This region of *SALL1* was found to be almost exactly identical to that of *SALL4* (data not shown). This finding prompted us to investigate whether *SALL4* was also able to bind β-catenin. We generated expression constructs of *SALL4A* and *SALL4B* tagged with hemagglutinin (HA). As shown in Figure 6A, endogenous β-catenin was pulled down by HA-*SALL4A* and HA-*SALL4B,* but not by HA alone.

Activation of the Wnt/β-catenin signaling pathway by both *SALL4A* and *SALL4B*

To investigate the functional effect of the interaction of the *SALL4* isoforms with β-catenin, we used a luciferase reporter (TOPflash; Upstate USA) containing multiple copies of Wnt-responsive elements to determine the potential of *SALL4A* and *SALL4B* to activate the canonical Wnt signaling pathway. The FOPflash reporter plasmid with mutated Wnt-response elements was used as a negative control. This reporter construct has been shown to be efficiently stimulated by Wnt1 in a variety of cell lines.[36-42] TOPflash or FOPflash reporter plasmid was transiently transfected in the HEK-293 cell line, in which both Wnt and its Wnt/β-catenin signal pathways were present. TOPflash reporter plasmid was also cotransfected with *SALL4A* or *SALL4B.* Significant activation of the Wnt/β-catenin signaling pathway by both *SALL4A* and *SALL4B* was indicated by increased luciferase activity in the TOPflash but not in the FOPflash reporter (Figure 6B).

Up-regulation of Wnt/β-catenin downstream target genes in *SALL4B* transgenic mice

We then studied the effect of overexpression of *SALL4B* on β-catenin/Tcf–dependent gene expression in *SALL4B* transgenic mice. Many genes are regulated by Wnt/β-catenin signaling pathway. We chose to study c-Myc and Cyclin D1 since both genes are transactivated by β-catenin/Tcf complex and involved in

Table 2. CBC from *SALL4B* transgenic mice and wild-type control

	n	WBC count, $\times 10^9$/L	Neutrophil count, $\times 10^9$/L	Lymphocyte count, $\times 10^9$/L	RBC count, $\times 10^{12}$/L	Hb level, g/L	Hematocrit	PLT count, $\times 10^9$/L
Transgenic mice	20	8.38 ± 1.76	0.93 ± 0.53	6.34 ± 2.31	8.85 ± 1.04	142.6 ± 15.2	.5052 ± .591	1616 ± 662
Control mice	18	11.59 ± 2.57	1.51 ± 0.43	9.04 ± 2.03	10.02 ± 0.92	156.6 ± 12.2	.5575 ± .481	1384 ± 806
P	—	.027	.048	.029	.015	.030	.038	.196

Plus-minus values indicate SD. Hb indicates hemoglobin; PLT, platelet; —, not applicable.

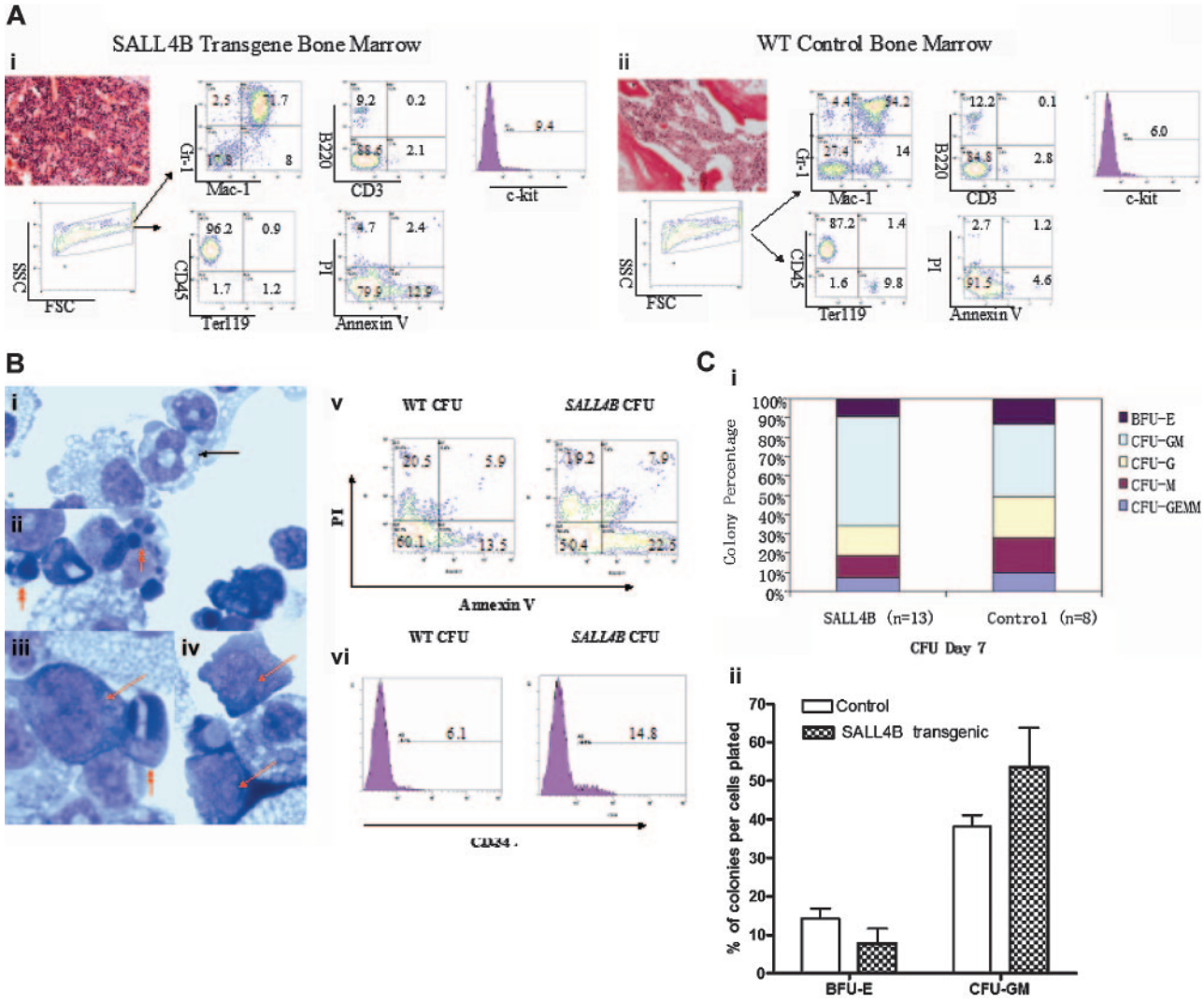

Figure 5. Ineffective hematopoiesis in *SALL4B* transgenic mice. (A) Comparison of bone marrow of *SALL4B* transgenic (i) and control mice (ii). *SALL4B* transgenic mouse bone marrow showed increased cellularity, myeloid population (Gr-1/Mac-1 double positive), immature population (c-kit positive), and apoptosis (annexin V positive, PI negative), compared with control WT mice. (B) Increased number of immature cells and apoptosis in CFUs from *SALL4B* transgenic mice. On day 7 of culture, a greater number of immature cells (ii-iv, red arrows) and apoptotic cells (ii-iv, double red arrows) were observed in transgenic mouse CFUs than in control CFUs (i). Consistent with this morphologic observation, there was increased apoptosis (annexin V positive, PI negative; v) and more $CD34^+$ immature cells (vi). (C) Comparison of bone marrow CFUs of *SALL4B* transgenic and control mice. Percentage of different types of colonies found in CFU assays of *SALL4B* transgenic and control mice (i). CFUs from *SALL4B* transgenic mice compared with control mice showed a statistically significant increase in CFU-GM (ii) (transgenic: 53.6 ± 10.3 [n = 13] vs WT: 38.1 ± 3.1 [n = 8]; $P = .002$) and decrease in BFU-E (transgenic: 7.8 ± 3.8 [n = 13] vs WT: 14.1 ± 2.7 [n = 8]; $P = .001$).

various human cancers including leukemia and lymphoma.[43] We found that in contrast to the wild-type controls, the mRNA expression of both genes was significantly up-regulated in preleukemia bone marrows and leukemic blasts from *SALL4B* transgenic mice (Figure 6C). These findings strengthen our hypothesis that *SALL4B* contributes to leukemogenesis, probably through activation of the Wnt/β-catenin signaling pathway.

Similar expression patterns of β-catenin and *SALL4* at different phases of CML

Dysregulated Wnt/β-catenin signaling is known to be involved in the development of LSCs. The best evidence for β-catenin's involvement in LSC self-renewal comes from the study of CML blast transformation. Jamieson et al[11] demonstrated that Wnt signaling was activated in the blast phase of CML but not the chronic phase, concluding that dysregulated Wnt signaling, such as activation of β-catenin, could confer the property of self-renewal on the GMPs of CML and lead to their blastic transformation. Given the potential interaction between *SALL4* and β-catenin and *spalt*'s position as a downstream target of Wnt signaling in *Drosophila*, we examined *SALL4* protein expression in CMLs in different phases. *SALL4* expression was present in blast-phase CML (n = 12, 75%) but not the chronic phase (n = 11 100%). In the accelerated phase (n = 6, 10%), in which blast counts are increased, immature blasts expressing *SALL4* were observed with a background of nonstaining more mature myeloid cells (data not shown).

Discussion

Homeobox and homeotic genes play important roles in normal development. Some homeobox genes, such as *Hox* and *Pax,* also function as oncogenes or as tumor suppressors in tumorigenesis or leukemogenesis. The important role of *SALL4,* a homeotic gene

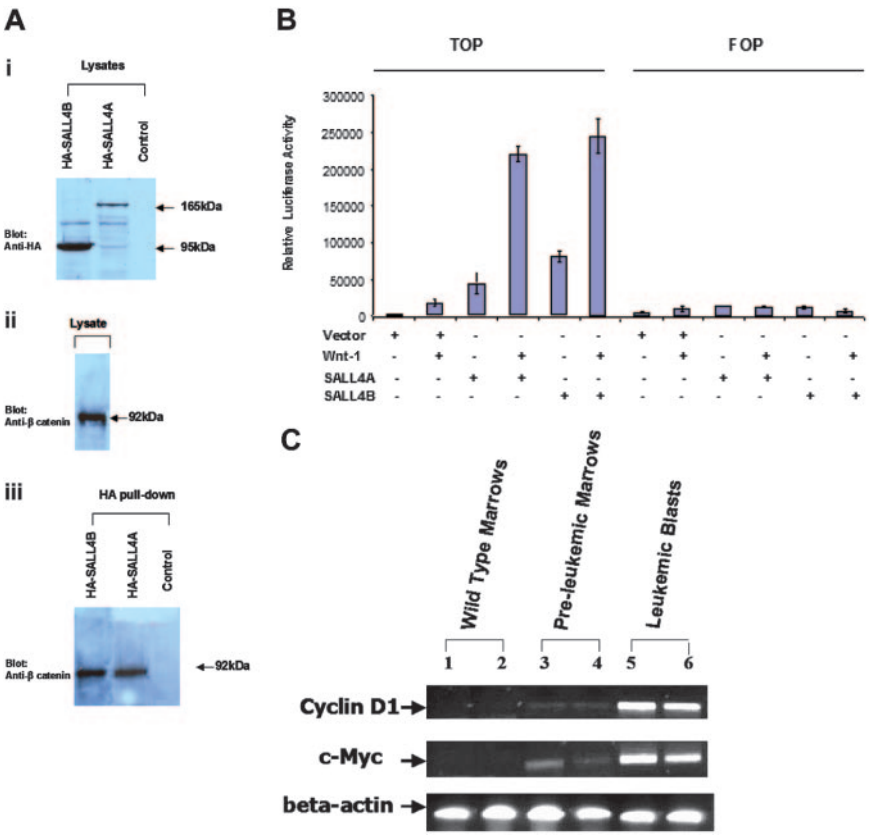

Figure 6. *SALL4* and the Wnt/β-catenin signaling pathway. (A) Both *SALL4A* and *SALL4B* can interact with β-catenin. Nuclear extracts (lysates) prepared from Cos-7 cells were transiently transfected with HA-*SALL4A* or HA-*SALL4B*. (i) Anti-HA antibody recognized both *SALL4A* (165 kDa) and *SALL4B* (95 kDa). (ii) β-Catenin was detected in the lysates. (iii) Immunoprecipitation was performed with the use of an HA affinity resin and detected with an anti–β-catenin antibody. β-Catenin was readily detected in both HA-*SALL4A* and HA-*SALL4B* pull-downs. Untransfected cells subjected to the same immunoprecipitation condition as the transfected cells were used as a control. (B) Activation of the Wnt/β-catenin signaling pathway by both *SALL4A* and *SALL4B*. HEK-293 cells were transfected with 1.0 μg of either mock alone, or *SALL4A* or *SALL4B* plasmid, with or without Wnt1 (including Wnt1, and its coactivators: LRP6, MESD, and $F_2$5), and TOPflash (TOP) or FOPflash (FOP) reporter plasmid (Upstate USA, Chicago, IL). After 24 hours, luciferase activity was measured. *SALL4A* or *SALL4B* alone showed more potent activation of Wnt signaling pathway when compared with the positive control Wnt1. In addition, both *SALL4* isoforms demonstrated a significantly synergistic activation of the Wnt signaling pathway with Wnt1. Data represent mean ± SD of 3 independent experiments. (C) Up-regulation of c-Myc and Cyclin D1 expression in *SALL4B* transgenic mice. RT-PCR analysis was performed on total bone marrow cells from 2 wild-type control mice (lanes 1-2), 2 preleukemic transgenic mice (lanes 3-4), and leukemic bone marrow cells from 2 leukemic transgenic *SALL4B* mice (lanes 5-6). Both c-Myc and Cyclin D1 expression were significantly up-regulated in *SALL4B* transgenic mice at both preleukemia MDS and leukemic stages. Beta actin was used as an internal standard.

and a transcriptional factor, in human development was recognized because heterozygous *SALL4* mutations lead to Duane-radial ray syndrome. *SALL4's* oncogenic role in leukemogenesis is described here for the first time.

We identified the 2 *SALL4* isoforms, *SALL4A* and *SALL4B*. During normal hematopoiesis, *SALL4* isoforms are expressed in the $CD34^+$ HSC/HPC population and rapidly turned off *(SALL4B)* or down-regulated *(SALL4A)* in normal human bone marrow and peripheral blood. In contrast, *SALL4* was constitutively expressed in all AML samples (n = 81) that we examined, and failed to turn off in human primary AML and myeloid leukemia cell lines. To directly test the leukemogenic potential of constitutive expression of *SALL4* in vivo, we generated *SALL4B* transgenic mice. The transgenic mice exhibited dysregulated hematopoiesis, much like that of human MDS, and AML that was transplantable. The MDS-like features in these *SALL4B* transgenic mice apparently did not require cooperating mutations and were observed as early as 2 months of age. The ineffective hematopoiesis observed in these mice was characterized, as it is in human MDS, by hypercellular bone marrow and paradoxic peripheral blood cytopenias (neutropenia and anemia) and dysplasia, which were probably secondary to the increased apoptosis noted in the bone marrow. The reason for the late onset of leukemia development in these transgenic mice may be the accumulation of additional genetic damage during the 8 or more months of replicative stress. Late onset of disease may also be a consequence of *SALL4*-induced genomic instability.

Our investigation of the potential mechanism of *SALL4* involvement in leukemogenesis demonstrated that both *SALL4A* and *SALL4B* interacted with β-catenin, an essential component of the Wnt signaling pathway involving self-renewal of HSCs. In addition, both were able to activate the Wnt/β-catenin pathway in a reporter gene assay, consistent with *SALL* family function in *Drosophila*[20,44] and humans.[30] Furthermore, similar to the situation with β-catenin, *SALL4* expression in CML varied at different phases of the disease: *SALL4* expression was absent in the chronic phase, became detectable in the accelerated phase only in immature blasts, and was strongly positive in the blast phase. The downstream target genes of Wnt/β-catenin, such as c-Myc and Cyclin D1, were up-regulated in *SALL4B* transgenic mice at both preleukemic and leukemic stages. On the basis of these studies, we propose a working hypothesis: constitutive expression of *SALL4* in AML may enable leukemic blasts to gain stem cell properties, such as self-renewal and/or lack of differentiation, and thus become LSCs.

In summary, the novel oncogene *SALL4* plays an important role in normal hematopoiesis and leukemogenesis. *SALL4B* transgenic mice exhibit MDS-like phenotype with subsequently AML transformation that is transplantable. Few animal models are currently available for the study of human MDS. The *SALL4B* transgenic mice that we generated provide a suitable animal model for understanding and treating human MDS and its subsequent transformation to AML. The interaction between *SALL4* and the Wnt/β-catenin signaling pathway not only provides a plausible mechanism for *SALL4* involvement in leukemogenesis but also advances our understanding of the activation of the Wnt/β-catenin signaling pathway in CML blastic transformation.

Acknowledgments

We gratefully acknowledge Dr Stephen Blacklow for making available Wnt plasmid constructs, Nikki Kong for immunohistochemical staining, and Dr Daniel G. Tenen and Dr David Ward for reviewing the paper.

References

1. Mufti G, List AF, Gore SD, Ho AY. Myelodysplastic syndrome. Hematology (Am Soc Hematol Educ Program). 2003:176-199.
2. Gilliland DG, Jordan CT, Felix CA. The molecular basis of leukemia. Hematology (Am Soc Hematol Educ Program). 2004:80-97.
3. Tenen DG. Disruption of differentiation in human cancer: AML shows the way. Nat Rev Cancer. 2003;3:89-101.
4. Rosmarin AG, Yang Z, Resendes KK. Transcriptional regulation in myelopoiesis: hematopoietic fate choice, myeloid differentiation, and leukemogenesis. Exp Hematol. 2005;33:131-143.
5. Friedman AD. Transcriptional regulation of myelopoiesis. Int J Hematol. 2002;75:466-472.
6. Gilliland DG. Molecular genetics of human leukemias: new insights into therapy. Semin Hematol. 2002;39:6-11.
7. Bonnet D, Dick JE. Human acute myeloid leukemia is organized as a hierarchy that originates from a primitive hematopoietic cell. Nat Med. 1997;3:730-737.
8. Huntly BJ, Gilliland DG. Blasts from the past: new lessons in stem cell biology from chronic myelogenous leukemia. Cancer Cell. 2004;6:199-201.
9. Huntly BJ, Gilliland DG. Leukaemia stem cells and the evolution of cancer-stem-cell research. Nat Rev Cancer. 2005;5:311-321.
10. Simon M, Grandage VL, Linch DC, Khwaja A. Constitutive activation of the Wnt/beta-catenin signalling pathway in acute myeloid leukaemia. Oncogene. 2005;24:2410-2420.
11. Jamieson CH, Ailles LE, Dylla SJ, et al. Granulocyte-macrophage progenitors as candidate leukemic stem cells in blast-crisis CML. N Engl J Med. 2004;351:657-667.
12. Reya T, Duncan AW, Ailles L, et al. A role for Wnt signalling in self-renewal of haematopoietic stem cells. Nature. 2003;423:409-414.
13. Reya T, Clevers H. Wnt signalling in stem cells and cancer. Nature. 2005;434:843-850.
14. Reya T. Regulation of hematopoietic stem cell self-renewal. Recent Prog Horm Res. 2003;58:283-295.
15. Staal FJ, Clevers HC. WNT signalling and haematopoiesis: a WNT-WNT situation. Nat Rev Immunol. 2005;5:21-30.
16. Kohlhase J, Schuh R, Dowe G, et al. Isolation, characterization, and organ-specific expression of two novel human zinc finger genes related to the Drosophila gene spalt. Genomics. 1996;38:291-298.
17. Kohlhase J, Hausmann S, Stojmenovic G, et al. SALL3, a new member of the human spalt-like gene family, maps to 18q23. Genomics. 1999;62:216-222.
18. Kohlhase J, Altmann M, Archangelo L, Dixkens C, Engel W. Genomic cloning, chromosomal mapping, and expression analysis of msal-2. Mamm Genome. 2000;11:64-68.
19. Al-Baradie R, Yamada K, St Hilaire C, et al. Duane radial ray syndrome (Okihiro syndrome) maps to 20q13 and results from mutations in SALL4, a new member of the SAL family. Am J Hum Genet. 2002;71:1195-1199.
20. Boube M, Llimargas M, Casanova J. Cross-regulatory interactions among tracheal genes support a co-operative model for the induction of tracheal fates in the Drosophila embryo. Mech Dev. 2000;91:271-278.
21. Mollereau B, Dominguez M, Webel R, et al. Two-step process for photoreceptor formation in Drosophila. Nature. 2001;412:911-913.
22. Ma Y, Li D, Chai L, et al. Cloning and characterization of two promoters for the human HSAL2 gene and their transcriptional repression by the Wilms tumor suppressor gene product. J Biol Chem. 2001;276:48223-48230.
23. Ma Y, Chai L, Cortez SC, et al. SALL1 expression in the human pituitary-adrenal/gonadal axis. J Endocrinol. 2002;173:437-448.
24. Ma Y, Singer DB, Gozman A, et al. Hsal 1 is related to kidney and gonad development and is expressed in Wilms tumor. Pediatr Nephrol. 2001;16:701-709.
25. Marlin S, Blanchard S, Slim R, et al. Townes-Brocks syndrome: detection of a SALL1 mutation hot spot and evidence for a position effect in one patient. Hum Mutat. 1999;14:377-386.
26. Nishinakamura R, Matsumoto Y, Nakao K, et al. Murine homolog of SALL1 is essential for ureteric bud invasion in kidney development. Development. 2001;128:3105-3115.
27. Kohlhase J, Schubert L, Liebers M, et al. Mutations at the SALL4 locus on chromosome 20 result in a range of clinically overlapping phenotypes, including Okihiro syndrome, Holt-Oram syndrome, acro-renal-ocular syndrome, and patients previously reported to represent thalidomide embryopathy. J Med Genet. 2003;40:473-478.
28. Kuhnlein RP, Frommer G, Friedrich M, et al. spalt encodes an evolutionarily conserved zinc finger protein of novel structure which provides homeotic gene function in the head and tail region of the Drosophila embryo. EMBO J. 1994;13:168-179.
29. Llimargas M. Wingless and its signalling pathway have common and separable functions during tracheal development. Development. 2000;127:4407-4417.
30. Sato A, Kishida S, Tanaka T, et al. Sall1, a causative gene for Townes-Brocks syndrome, enhances the canonical Wnt signaling by localizing to heterochromatin. Biochem Biophys Res Commun. 2004;319:103-113.
31. Arroyo JL, Fernandez ME, Hernandez JM, Orfao A, San Miguel JF, del Canizo MC. Impact of immunophenotype on prognosis of patients with myelodysplastic syndromes: its value in patients without karyotypic abnormalities. Hematol J. 2004;5:227-233.
32. Buonamici S, Li D, Chi Y, et al. EVI1 induces myelodysplastic syndrome in mice. J Clin Invest. 2004;114:713-719.
33. Cuenco GM, Nucifora G, Ren R. Human AML1/MDS1/EVI1 fusion protein induces an acute myelogenous leukemia (AML) in mice: a model for human AML. Proc Natl Acad Sci U S A. 2000;97:1760-1765.
34. Lin YW, Slape C, Zhang Z, Aplan PD. NUP98-HOXD13 transgenic mice develop a highly penetrant, severe myelodysplastic syndrome that progresses to acute leukemia. Blood. 2005;106:287-295.
35. Marisavljevic D, Rolovic Z, Sefer D, et al. Biological and clinical significance of clonogenic assays in patients with myelodysplastic syndromes. Med Oncol. 2002;19:249-259.
36. Cullen DA, Killick R, Leigh PN, Gallo JM. The effect of polyglutamine expansion in the human androgen receptor on its ability to suppress beta-catenin-Tcf/Lef dependent transcription. Neurosci Lett. 2004;354:54-58.
37. Dong Y, Drissi H, Chen M, et al. Wnt-mediated regulation of chondrocyte maturation: modulation by TGF-beta. J Cell Biochem. 2005;95:1057-1068.
38. Esufali S, Bapat B. Cross-talk between Rac1 GTPase and dysregulated Wnt signaling pathway leads to cellular redistribution of beta-catenin and TCF/LEF-mediated transcriptional activation. Oncogene. 2004;23:8260-8271.
39. Holmen SL, Salic A, Zylstra CR, Kirschner MW, Williams BO. A novel set of Wnt-Frizzled fusion proteins identifies receptor components that activate beta -catenin-dependent signaling. J Biol Chem. 2002;277:34727-34735.
40. Merdek KD, Nguyen NT, Toksoz D. Distinct activities of the alpha-catenin family, alpha-catulin and alpha-catenin, on beta-catenin-mediated signaling. Mol Cell Biol. 2004;24:2410-2422.
41. You L, He B, Xu Z, et al. Inhibition of Wnt-2-mediated signaling induces programmed cell death in non-small-cell lung cancer cells. Oncogene. 2004;23:6170-6174.
42. Warner DR, Greene RM, Pisano MM. Cross-talk between the TGFbeta and Wnt signaling pathways in murine embryonic maxillary mesenchymal cells. FEBS Lett. 2005;579:3539-3546.
43. Luu HH, Zhang R, Haydon RC, et al. Wnt/beta-catenin signaling pathway as a novel cancer drug target. Curr Cancer Drug Targets. 2004;4:653-671.
44. Ribeiro C, Neumann M, Affolter M. Genetic control of cell intercalation during tracheal morphogenesis in Drosophila. Curr Biol. 2004;14:2197-2207.

2006 108: 2726-2735
doi:10.1182/blood-2006-02-001594 originally published online June 8, 2006

SALL4, a novel oncogene, is constitutively expressed in human acute myeloid leukemia (AML) and induces AML in transgenic mice

Yupo Ma, Wei Cui, Jianchang Yang, Jun Qu, Chunhui Di, Hesham M. Amin, Raymond Lai, Jerome Ritz, Diane S. Krause and Li Chai

Blood (print ISSN 0006-4971, online ISSN 1528-0020), is published weekly by the American Society of Hematology, 2021 L St, NW, Suite 900, Washington DC 20036.